International Atomic Energy Agency

INDC(CCP)-379
Distr.: L

INDC INTERNATIONAL NUCLEAR DATA COMMITTEE

RESULTS OF RELATIVE MEASUREMENTS OF PHOTOFISSION YIELDS AND CROSS-SECTIONS FOR $^{233,235}U$, ^{237}Np, $^{239,241}Pu$ AND ^{241}Am NUCLEI IN THE 5-11 MeV REGION

A.S. Soldatov and G.N. Smirenkin
Institute of Physics and Power Engineering, Obninsk, Russia

(Translated from a Russian original published in
Yadernye Konstanty 3-4/1992, p. 59-70)

Translated by the IAEA

August 1994

Reproduced by the IAEA in Austria
August 1994

INDC(CCP)-379
Distr.: L

94-10590 (10)
Translated from Russian

UDC 539.173

RESULTS OF RELATIVE MEASUREMENTS OF PHOTOFISSION YIELDS AND CROSS-SECTIONS FOR $^{233,235}U$, ^{237}Np, $^{239,241}Pu$ AND ^{241}Am NUCLEI IN THE 5-11 MeV REGION

A.S. Soldatov and G.N. Smirenkin

Institute of Physics and Power Engineering, Obninsk

ABSTRACT

The authors present the results of relative measurements of photofission yield for a group of odd nuclei from ^{233}U to ^{241}Am (relative to ^{238}U photofission yield) in the region of limit energies of the bremsstrahlung spectrum E_{max} = 7-11 MeV. The photofission cross-sections unfolded from them are given for the group (6) of nuclei studied, together with the evaluated photofission cross-section for ^{238}U, which is used as the standard.

The present paper, like Ref. [3], presents detailed numerical data on the photofission yields and cross-sections of six A-odd nuclei from ^{233}U to ^{241}Am in the 5-11 MeV photon energy region, which were described in Ref. [3]. The measurements were carried out in an extracted electron beam on the microtron at the Institute for Physical Problems using fission fragment track detectors. Part of the results considered in Ref. [3] appeared in Refs [1, 2] (E_{max} = 5-7 MeV), while the remainder (up to 11 MeV) are published for the first time here[1] as well as in Ref. [3]. In this paper we briefly deal with the formulation of the problem, giving the methodology and results of the study [3] to the extent needed to clarify the information given below.

---

[1] There has been a long delay in deriving the information obtained earlier by means of visual track detector counting.

1. The quantity which is measured directly in the experimental study of the photofission probability of nuclei in bremsstrahlung beams is yield $Y(E_{max})$, which can be defined as the number of fission events (relative to unit mass of fissile material and unit electron current) in a target at a distance r from the source, and which can be written as [3]

$$Y(E_{max}) = C(E_{max}) \int_{o}^{E_{max}} \sigma_f(E)\, N(E,E_{max})\, dE\,, \tag{1}$$

$$C(E_{max}) = \frac{N_o}{A} \frac{I_o(E_{max})}{4\pi r^2}\,, \tag{2}$$

where $\sigma_f(E)$ is the photofission cross-section, $E_{max} = E_e$ the limit energy in the bremsstrahlung spectrum $N(E,E_{max})$ equal to electron kinetic energy E_e, N_0 is the Avogadro number, $I_0(E_{max})$ the integral (integrated over all photon energies E) bremsstrahlung intensity in the direction $\nu = 0°$ with respect to the electron beam[2].

Use of the relative method enables us to do away with laborious measurements of beam intensity $I_0(E_{max})$ (or photon flux to the sample $I_0/4\pi r^2$) and to replace the absolute measurements of the mass of fissile material by much simpler relative measurements. In Ref. [3], as in many other studies, the standard used for such measurements was ^{238}U, whose photofission cross-section $\sigma^0_f(E)$ has been more extensively studied than that of other nuclei.

2. In Ref. [3] we do not simply combine data sets in two neighbouring energy ranges but introduce a number of refinements into the values given in Refs [1, 2]. These relate to determination of the ratios of photofission yields of the nuclei studied and ^{238}U, and to unfolding of cross-sections $\sigma_f(E)$ from them.

---

[2] The presence of integral radiation intensity $I_0(E_{max})$ ensures normalization of spectrum $N(E,E_{max})$ to unity.

$$R(E_{max}) = \frac{Y(E_{max})}{Y_o(E_{max})} = \frac{\int_o^{E_{max}} \sigma_f(E)\, N(E,E_{max})\, dE}{\int_o^{E_{max}} \sigma_f^o(E)\, N(E,E_{max})\, dE}. \qquad (3)$$

One such refinement involves finding the values of electron energy $E_e = E_{max}$. A more accurate consideration of electron energy losses during passage through the sealing of the electron conductor foil has led to a small energy shift, on an average by 25 keV, towards the lower values, as compared with Refs [1, 2] [3]. All the values for $R(E_{max})$ from the present paper and from Refs [1, 2] are given in Table 1 and Fig. 1, where they are also compared with other experimental data [4, 5].

3. The above-mentioned sensitivity of the cross-sections under determination to energy correction is to a considerable extent due to the nonmonotonic nature (resonance structure) of the standard cross-section $\sigma^0_f(E)$ in the fission threshold region ($E \leq 6$ MeV). This is, undoubtedly, a disadvantage of the ^{238}U photofission cross-section as a standard for relative measurements, and might give rise to an incorrect structure in the energy dependence of the cross-sections $\sigma_f(E)$ under determination. For this reason considerable attention was paid in Ref. [3] to evaluating cross-section $\sigma^0_f(E)$. We note that the choice of the photofission cross-sections of odd nuclei as the subject of study in Ref. [3] is also associated with testing of the recommended curve $\sigma^0_f(E)$.

The origin of the cross-section resonance structure in the near-threshold energy region is linked with quasi-stationary states of the vibration type in the second well of the fission

---

[3] Although the given correction is comparable with the energy resolution of the electron beam, consideration of this correction has a marked effect in subsequent processing of experimental data on $R(E_{max})$.

barrier Refs [6, 7]. These effects are strongly dependent on the parity of the fissioning nucleus; they are most marked in even-even nuclei (for example, ^{238}U) and are much weaker in odd nuclei. In the latter case, the density of internal excitations is greater and so is the vibration mode damping determined by it. Smoothness of the energy dependence of the cross-sections for odd nuclei was the property by which the evaluated curve $\sigma^0_f(E)$ was tested. It is shown in Fig. 2. The numerical data for $\sigma^0_f(E)$ are given in Table 2.

As previously, we used Tarasko's method of minimizing the directed divergence [15] to unfold the photofission cross-sections of the investigated nuclei from Eq. (3), which is an incorrectly posed problem. In determining $\sigma_f(E)$, the results of calculating the bremsstrahlung spectrum from a thick tungsten target Ref. [16] were analytically approximated as in Ref. [17]. The results of the mathematical treatment, in which we basically followed Ref. [1], including calculation of errors $\Delta\sigma_f(E)$, are shown in Table 3, and also on Figs 3 and 4. In Fig. 3 the absence of systematic correlations between irregularities of $\sigma_f(E)$ in the vicinity of the dotted vertical lines denoting resonances of $\sigma^0_f(E)$ indicates, in particular, that the difficulties in using the ^{238}U photofission cross-section as a standard for relative measurements were overcome.

REFERENCES

[1] ZHUCHKO, V.E., et al., Yad. Fiz. 28 (1978) 1170.

[2] OSTAPENKO, Yu.B., et al., in: Problems of Atomic Science and Technology, Ser. Nuclear Constants, No. 3, 30 (1978) 3 (in Russian).

[3] SOLDATOV, A.S., SMIRENKIN, G.N., Yad. Fiz. 55 2 (1992) 763.

[4] IVANOV, K.N. and PETRZHAK, K.A., At. Ehnerg. 36 (1974) 404.

[5] ALEKSANDROV, B.M., et al., Yad. Fiz. 43 (1986) 290.

[6] BJORNHOLM, S., STRUTINSKY, V.M., Nucl. Phys. A136 (1969) 1.

[7] BJORNHOLM, S., LYNN, J.E., Rev .Mod. Phys. 52 (1980) 725.

[8] CALDWELL, J.T., et al., Phys. Rev. C21 (1980) 1215.

[9] DICKEY, P.A., AXEL, P., Phys. Rev. Lett. 35 (1975) 501.

[10] KNOWLES, J.W., MAFRA, O.Y., in: Proc. of the Intern. Conf. on Photonuclear Reaction and Application, Asilomar, California, 5D7-1.

[11] HAWKES, N.P., AERE R-12675, UKAEA, Harwell (1986).

[12] KATZ, L., et al., in: Proc. of Second UN Conf. on the PUAE, US, Geneva, 15 (1958) 188.

[13] VEYSSIERE, A., et al., Nucl. Phys. A199 (1973) 45.

[14] RIES, H., et al., Phys. Rev. C29 (1984) 2346.

[15] TARASKO, M.Z., "Method of minimizing the directed divergence in problems of determination of distributions" Preprint FEhI-1446, Obninsk (1983) (in Russian).

[16] ZHUCHKO, V.E., and TSIPENYUK, Yu.M., At. Ehnerg. 39 (1975) 66.

[17] TARASKO, M.Z., et al., At. Ehnerg. 65 (1988) 290.

[18] BERMAN, B.J., et al., Phys. Rev. C34 (1986) 2201.

[19] KORETSKAYA, I.S., et al., Yad. Fiz. 30 (1979) 910.

Table 1

Ratios R of photofission reaction yields of the investigated nuclei to the photofission yield of the standard ^{238}U as a function of bremsstrahlung spectrum limit energy E_{max}

E_{max}, MeV	^{233}U	^{235}U	^{237}Np	^{239}Pu	^{241}Pu	^{241}Am
4.975	0.49±0.08	0.04±0.01	2.68±0.08	2.04±0.12	3.13±0.32	5.92±0.27
5.075	0.59±0.04	0.06±0.01	2.46±0.05	1.98±0.08	3.30±0.12	4.75±0.18
5.175	2.04±0.17	0.13±0.01	3.27±0.06	2.35±0.19	4.02±0.33	4.09±0.33
5.275	4.51±0.14	0.26±0.01	4.18±0.07	2.90±0.09	4.34±0.13	3.89±0.12
5.375	5.46±0.14	0.38±0.01	3.91±0.09	2.97±0.08	3.52±0.09	3.16±0.07
5.475	6.46±0.14	0.61±0.01	4.33±0.09	3.40±0.07	2.92±0.06	3.01±0.07
5.575	5.51±0.12	0.67±0.01	4.25±0.09	3.31±0.07	1.91±0.04	2.49±0.06
5.675	4.10±0.24	0.58±0.03	3.48±0.07	2.45±0.14	1.23±0.07	1.84±0.11
5.775	3.47±0.08	0.60±0.01	3.20±0.07	2.17±0.04	0.98±0.02	1.63±0.04
5.875	3.35±0.06	0.74±0.01	3.27±0.07	2.04±0.04	0.97±0.02	1.67±0.03
5.975	3.16±0.06	0.87±0.02	3.24±0.07	1.92±0.04	0.98±0.02	1.80±0.03
6.075	2.81±0.07	0.91±0.02	2.96±0.06	1.72±0.04	0.97±0.02	1.81±0.05
6.175	2.54±0.13	0.93±0.05	2.79±0.06	1.39±0.07	0.92±0.07	1.79±0.13
6.275	2.21±0.05	0.96±0.02	2.59±0.05	1.38±0.03	0.98±0.02	1.83±0.09
6.375	2.08±0.05	0.98±0.02	2.55±0.05	1.35±0.03	1.00±0.02	1.92±0.09
6.475	2.04±0.06	1.01±0.03	2.53±0.05	1.35±0.03	1.03±0.03	1.99±0.10
6.575	1.98±0.07	1.07±0.04	2.53±0.05	1.38±0.03	1.08±0.04	2.14±0.11
6.675	1.94±0.04	1.11±0.02	2.54±0.05	1.39±0.03	1.14±0.02	2.21±0.05
6.775	1.89±0.04	1.14±0.02	2.56±0.05	1.41±0.03	1.13±0.02	2.27±0.05
6.875	1.99±0.04	1.15±0.02	2.54±0.05	1.46±0.04	1.19±0.03	2.36±0.05
6.975	1.94±0.04	1.18±0.02	2.53±0.05	1.48±0.03	1.21±0.02	2.37±0.05
7.075	1.90±0.04	1.19±0.02	2.48±0.05	1.49±0.03	1.22±0.02	2.44±0.05
7.175	1.89±0.04	1.23±0.03	2.57±0.05	1.50±0.03	1.24±0.03	2.48±0.05
7.275	1.99±0.04	1.29±0.03	2.63±0.05	1.54±0.03	1.26±0.03	2.54±0.06

Table 1 (continued)

E_{max}, MeV	^{233}U	^{235}U	^{237}Np	^{239}Pu	^{241}Pu	^{241}Am
7.375	1.97±0.04	1.30±0.03	2.61±0.05	1.55±0.03	1.27±0.03	2.61±0.06
7.475	1.99±0.04	1.31±0.03	2.61±0.05	1.61±0.03	1.30±0.03	2.61±0.06
7.575	1.95±0.04	1.33±0.03	2.52±0.05	1.62±0.03	1.29±0.03	2.62±0.06
7.675	1.97±0.04	1.32±0.03	2.59±0.05	1.61±0.03	1.36±0.03	2.67±0.06
7.775	2.00±0.04	1.37±0.03	2.55±0.05	1.68±0.03	1.37±0.03	2.64±0.06
7.875	1.92±0.04	1.35±0.03	2.50±0.05	1.64±0.03	1.36±0.03	2.62±0.06
7.975	2.03±0.04	1.38±0.03	2.63±0.05	1.74±0.03	1.38±0.03	2.80±0.06
8.075	2.04±0.04	1.43±0.03	2.62±0.05	1.72±0.03	1.38±0.03	2.79±0.06
8.175	2.01±0.04	1.40±0.03	2.62±0.05	1.73±0.03	1.37±0.03	2.75±0.06
8.275	2.05±0.04	1.45±0.03	2.63±0.05	1.77±0.04	1.39±0.03	2.87±0.06
8.375	2.03±0.04	1.44±0.03	2.71±0.05	1.79±0.04	1.35±0.03	2.98±0.07
8.475	2.08±0.04	1.45±0.03	2.61±0.05	1.84±0.04	1.38±0.03	2.92±0.06
8.575	2.13±0.04	1.46±0.03	2.68±0.05	1.88±0.04	1.41±0.03	3.01±0.07
8.675	2.12±0.04	1.48±0.03	2.63±0.05	1.93±0.04	1.42±0.03	3.05±0.07
8.775	2.14±0.04	1.49±0.03	2.63±0.05	1.91±0.04	1.42±0.03	3.02±0.07
8.875	2.14±0.04	1.50±0.03	2.68±0.05	1.95±0.04	1.41±0.03	2.99±0.07
8.975	2.09±0.04	1.48±0.03	2.58±0.05	1.95±0.04	1.42±0.03	2.95±0.07
9.075	2.12±0.04	1.51±0.03	2.58±0.05	1.98±0.04	1.41±0.03	2.95±0.07
9.175	2.11±0.04	1.51±0.03	2.57±0.05	1.99±0.04	1.42±0.03	3.00±0.07
9.275	2.14±0.04	1.53±0.03	2.54±0.05	1.98±0.04	1.43±0.03	3.00±0.07
9.375	2.12±0.04	1.49±0.03	2.57±0.05	2.01±0.04	1.43±0.03	3.03±0.07
9.475	2.16±0.04	1.55±0.03	2.59±0.05	1.98±0.04	1.44±0.03	3.01±0.07
9.575	2.13±0.04	1.58±0.03	2.58±0.05	2.03±0.04	1.45±0.03	3.07±0.07
9.675	2.16±0.04	1.57±0.03	2.51±0.05	2.04±0.04	1.45±0.03	2.96±0.07

Table 1 (continued)

E_{max}, MeV	^{233}U	^{235}U	^{237}Np	^{239}Pu	^{241}Pu	^{241}Am
9.775	2.18±0.04	1.57±0.03	2.57±0.05	2.03±0.04	1.46±0.03	2.95±0.07
9.875	2.20±0.04	1.60±0.03	2.57±0.05	2.05±0.04	1.46±0.03	3.04±0.07
9.975	2.23±0.05	1.61±0.03	2.59±0.05	2.08±0.04	1.47±0.03	3.02±0.07
10.075	2.20±0.04	1.58±0.03	2.57±0.05	2.10±0.04	1.47±0.03	3.06±0.07
10.175	2.20±0.04	1.62±0.03	2.54±0.05	2.12±0.04	1.47±0.03	3.08±0.07
10.275	2.22±0.04	1.67±0.03	2.60±0.05	2.15±0.04	1.51±0.03	3.03±0.07
10.375	2.22±0.04	1.69±0.03	2.57±0.05	2.17±0.04	1.51±0.03	2.99±0.07
10.475	2.25±0.05	1.67±0.03	2.59±0.05	2.17±0.04	1.48±0.03	2.92±0.07
10.575	2.23±0.04	1.65±0.03	2.57±0.05	2.13±0.04	1.51±0.03	2.94±0.07
10.675	2.23±0.05	1.69±0.03	2.59±0.05	2.17±0.04	1.52±0.03	3.01±0.07
10.775	2.21±0.04	1.66±0.03	2.62±0.05	2.17±0.04	1.52±0.03	3.01±0.07
10.875	2.21±0.04	1.71±0.03	2.65±0.05	2.18±0.04	1.55±0.03	2.99±0.07
10.975	2.24±0.05	1.73±0.04	2.64±0.05	2.21±0.04	1.53±0.03	2.97±0.07

Table 2

Standard photofission cross-section $\sigma^0(^{238}U)$ in millibarns

E, MeV	^{238}U	E, MeV	^{238}U	E, MeV	^{238}U
5.0	0.021	7.4	12.5	9.8	59.9
5.1	0.047	7.5	13.0	9.9	63.5
5.2	0.063	7.6	13.7	10.0	68.1
5.3	0.280	7.7	14.3	10.1	72.7
5.4	0.345	7.8	15.0	10.2	77.3
5.5	0.850	7.9	16.0	10.3	81.8
5.6	2.85	8.0	17.0	10.4	86.5
5.7	4.10	8.1	18.1	10.5	91.2
5.8	3.25	8.2	19.2	10.6	95.6
5.9	2.97	8.3	20.4	10.7	99.4
6.0	6.25	8.4	21.7	10.8	102.2
6.1	8.10	8.5	23.0	10.9	103.4
6.2	8.85	8.6	24.3	11.0	103.6
6.3	7.50	8.7	25.6	11.1	102.7
6.4	6.80	8.8	26.9	11.2	101.7
6.5	6.40	8.9	28.4	11.3	100.6
6.6	6.80	9.0	30.3	11.4	99.6
6.7	7.97	9.1	32.2	11.5	98.7
6.8	9.37	9.2	34.5	11.6	97.8
6.9	10.8	9.3	37.3	11.7	97.4
7.0	11.4	9.4	40.7	11.8	97.5
7.1	11.5	9.5	45.0	11.9	98.3
7.2	11.8	9.6	49.7	12.0	99.5
7.3	12.1	9.7	54.3	12.1	101.2

Table 3

Photofission cross-sections σ of the investigated nuclei in millibarns

E, MeV	^{233}U	^{235}U	^{237}Np	^{239}Pu	^{241}Pu	^{241}Am
5.0	0.01±0.003	0.002±0.001	0.05±0.02	0.04±0.01	0.05±0.01	0.08±0.02
5.1	0.14±0.02	0.008±0.003	0.17±0.03	0.12±0.01	0.20±0.02	0.13±0.02
5.2	0.77±0.08	0.040±0.006	0.50±0.04	0.32±0.04	0.42±0.07	0.30±0.05
5.3	1.45±0.07	0.11 ±0.008	0.78±0.08	0.69±0.06	0.60±0.06	0.55±0.09
5.4	3.20±0.13	0.34 ±0.024	2.00±0.16	1.63±0.10	0.75±0.05	1.10±0.09
5.5	4.90±0.20	0.83 ±0.042	4.60±0.23	3.34±0.14	0.87±0.06	2.10±0.17
5.6	7.10±0.34	1.31 ±0.07	7.60±0.38	4.63±0.28	1.35±0.12	3.25±0.29
5.7	8.35±0.84	2.30 ±0.30	8.90±0.50	5.20±0.68	2.05±0.29	4.50±0.58
5.8	8.70±0.96	4.40 ±0.35	11.2±1.5	4.88±0.49	3.30±0.46	6.50±0.78
5.9	8.35±0.42	6.10 ±0.36	11.4±1.2	4.39±0.35	4.45±0.36	9.20±0.64
6.0	7.70±0.39	6.80 ±0.36	11.5±1.2	4.31±0.47	5.65±0.40	11.5±1.0
6.1	7.70±0.47	7.60 ±0.76	13.0±2.0	4.71±0.57	7.00±0.70	14.0±1.5
6.2	8.10±0.70	8.70 ±0.87	14.2±1.6	7.40±0.85	9.40±1.00	17.4±1.9
6.3	9.40±1.00	9.60 ±0.96	16.5±1.8	10.2±1.3	10.4±1.1	20.7±2.3
6.4	11.4±1.2	10.45±1.1	18.4±1.9	12.0±1.2	11.2±1.2	23.0±2.5
6.5	13.2±1.4	11.6 ±1.2	20.1±2.1	13.8±1.4	11.9±1.2	24.5±2.7
6.6	15.3±1.6	12.4 ±1.3	21.7±2.2	14.9±1.5	12.5±1,3	25.3±2.8
6.7	17.5±1.8	13.2 ±1.4	23.2±2.4	16.2±1.7	13.2±1.3	26.5±2.9
6.8	19.4±2.0	14.4 ±1.5	24.8±2.5	17.5±1.8	14.1±1.4	28.2±3.1
6.9	20.8±2.1	16.0 ±1.6	26.8±2.7	18.6±1.9	15.0±1.5	30.1±3.3
7.0	22.6±2.3	17.6 ±1.8	28.9±2.9	20.2±2.1	16.0±1.6	32.3±3.6
7.1	25.0±2.5	19.1 ±2.0	30.8±3.1	21.7±2.2	17.2±1.7	34.3±3.8
7.2	26.1±2.6	20.0 ±2.0	31.6±3.2	23.5±2.4	18.2±1.8	36.3±4.0
7.3	27.1±2.7	20.6 ±2.1	32.4±3.3	25.2±2.6	19.2±1.9	38.2±4.2

Table 3 (continued)

E, MeV	^{233}U	^{235}U	^{237}Np	^{239}Pu	^{241}Pu	^{241}Am
7.4	28.2±2.9	21.3±2.2	33.7±3.4	26.9±2.7	20.0±2.0	40.3±4.4
7.5	30.0±3.0	22.3±2.3	35.6±3.6	28.5±2.9	20.8±2.1	43.2±4.7
7.6	31.5±3.2	23.4±2.4	38.0±4.0	30.5±3.1	21.5±2.2	46.6±5.0
7.7	33.7±3.4	24.7±2.5	40.7±4.1	32.9±3.3	21.9±2.2	50.6±5.3
7.8	36.0±3.7	26.2±2.7	43.0±4.3	35.6±3.6	22.4±2.3	55.3±5.7
7.9	38.2±4.0	28.0±2.8	45.6±4.6	38.5±3.9	23.2±2.3	59.5±6.1
8.0	40.8±4.2	29.0±2.9	47.0±4.7	41.2±4.2	24.3±2.5	62.4±6.5
8.1	42.0±4.3	30.5±3.1	48.0±5.0	43.9±4.4	25.7±2.6	65.5±7.2
8.2	45.3±4.7	32.0±3.5	49.7±5.0	47.7±4.8	27.5±2.8	68.2±7.5
8.3	48.0±4.9	34.0±3.5	50.2±5.1	50.8±5.1	29.6±3.0	69.5±7.8
8.4	50.0±5.2	36.0±3.6	51.5±5.2	53.5±5.4	31.9±3.2	70.3±8.1
8.5	52.0±5.5	38.5±3.9	53.3±5.4	55.7±5.6	34.1±3.4	71.5±8.5
8.6	53.5±5.7	41.0±4.0	55.4±5.5	57.3±5.8	36.1±3.6	72.6±8.8
8.7	56.2±5.9	43.5±4.5	58.0±5.9	59.2±6.0	38.2±4.0	74.8±9.1
8.8	59.0±6.3	47.0±4.9	61.0±6.2	61.8±6.3	41.0±4.3	78.5±9.8
8.9	63.7±7.1	51.0±5.3	65.5±6.7	65.4±6.6	44.0±4.5	84.0±10.5
9.0	69.3±8.0	55.5±5.7	71.5±7.4	69.9±7.1	48.0±5.2	90.8±11.0
9.1	75.5±3.5	61.0±6.3	79.0±8.0	74.8±8.0	52.0±5.6	97.5±12.0
9.2	82.7±9.2	67.0±6.9	87.0±9.2	81.3±8.7	56.5±6.0	105 ±14.0
9.3	90.5±10	73.7±7.5	95.5±10.0	88.6±9.1	62.0±6.7	113 ±16.0
9.4	99.0±11	81.0±9.0	105 ±11.6	96.7±10.8	67.0±7.5	121 ±17.0
9.5	108 ±14	89.5±10.4	115 ±13.0	106 ±12.5	73.0±9.0	130 ±18.0
9.6	118 ±15	96.0±11.2	128 ±15.0	117 ±14.0	79.5±9.5	141 ±20.0
9.7	127 ±16	105 ±13.0	142 ±16.7	129 ±15.5	86.0±10.	155 ±22.0

Table 3 (continued)

E, MeV	^{233}U	^{235}U	^{237}Np	^{239}Pu	^{241}Pu	^{241}Am
9.8	136±17	115±13.7	155±19.0	142±17.0	93.5±11.0	168±24.0
9.9	145±18	125±15	169±20.0	153±19.0	103 ±12.3	179±26.0
10.0	154±20	136±17	184±22.0	164±21.0	112 ±14.0	190±27.0
10.1	164±22	146±19	199±26.0	173±23.0	120 ±16.0	200±31.0
10.2	174±25	153±22	213±30.0	182±26.0	130 ±19.0	212±34.0
10.3	184±28	158±24	226±35.0	190±29.0	138 ±21.0	227±39.0
10.4	192±32	163±26	238±38.0	200±33.0	145 ±24.0	247±46.0
10.5	202±33	172±27	251±43.0	210±35.0	153 ±26.0	267±53.0
10.6	214±39	182±33	260±47.0	221±40.0	160 ±29.0	283±59.0
10.7	227±46	189±37	265±50.0	231±45.0	167 ±32.0	293±65.0
10.8	241±52	196±39	268±54.0	244±51.0	175 ±35.0	302±72.0
10.9	254±58	201±42	270±56.0	256±54.0	180 ±38.0	310±75.0

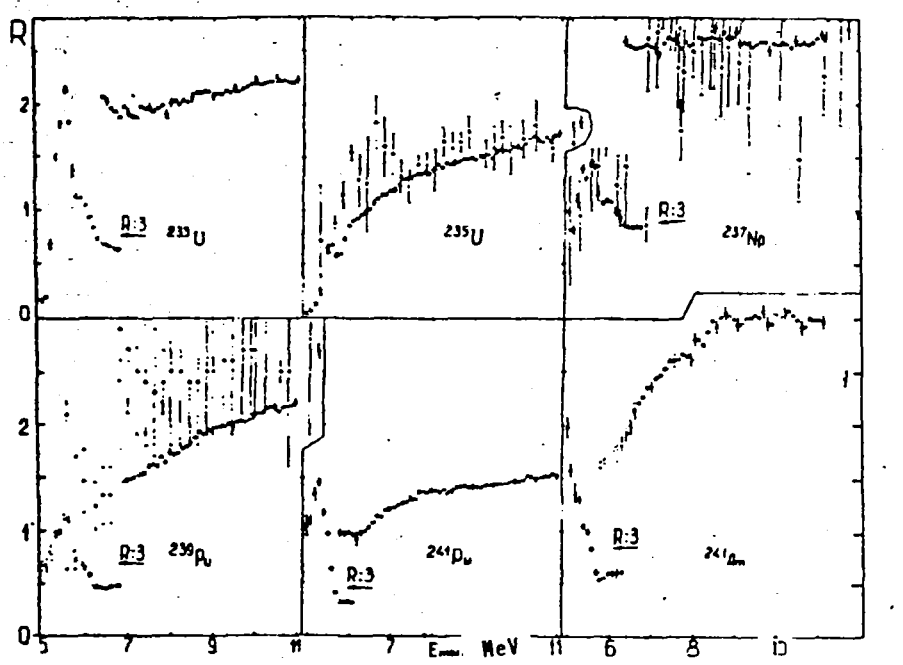

Fig. 1. Ratios R of photofission yields for the investigated nuclei and the ^{238}U nucleus as a function of the bremsstrahlung spectrum limit energy E_{max}. Experimental data: o - present study, + - Ref. [4], • - Ref. [5]. For $E_{max} \leq 6.5$ MeV the values given have been reduced by a factor of 3.

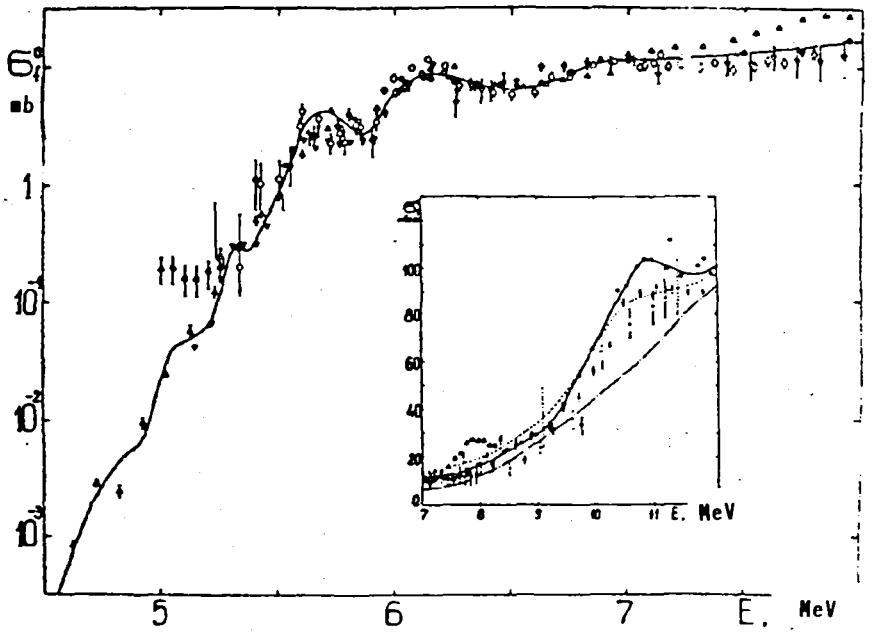

Fig. 2. ^{238}U photofission cross-section $\sigma^0_f(E)$ near the threshold. On the inset $\sigma^0_f(E)$ is on the left-hand slope of the giant resonance. Evaluation of $\sigma^0_f(E)$: -. Experimental data: ▲ - Ref. [1, 2], ⊗ - Ref. [8], o - Ref. [9], △ - Ref. [10], ∇ - Ref. [11], _·_ - Ref. [12], x - Ref. [13], + - Ref. [14].

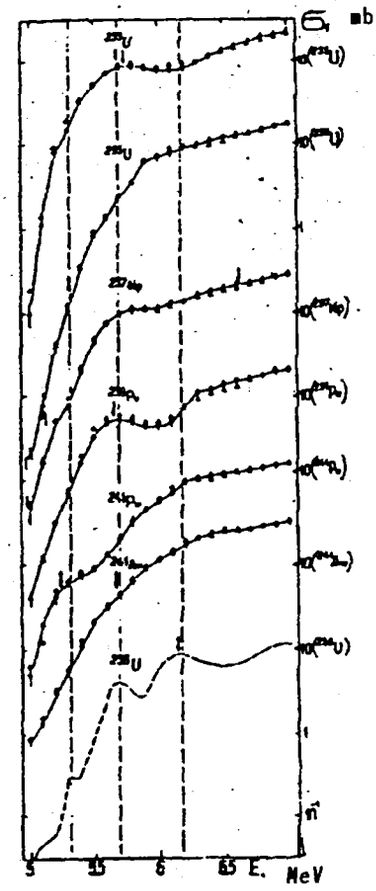

Fig. 3. Comparison of unfolded photofission cross-sections for the investigated nuclei with the evaluated cross-section curve for the standard (^{238}U). o denotes cross-sections obtained using experimental data on $R(E_{max})$ ratios and the evaluated curve of the standard $\sigma^0_f(E)$ and ▲ there obtained using the corrected experimental yields [1, 2]. The arrows show the neutron binding energies. The scale is logarithmic.

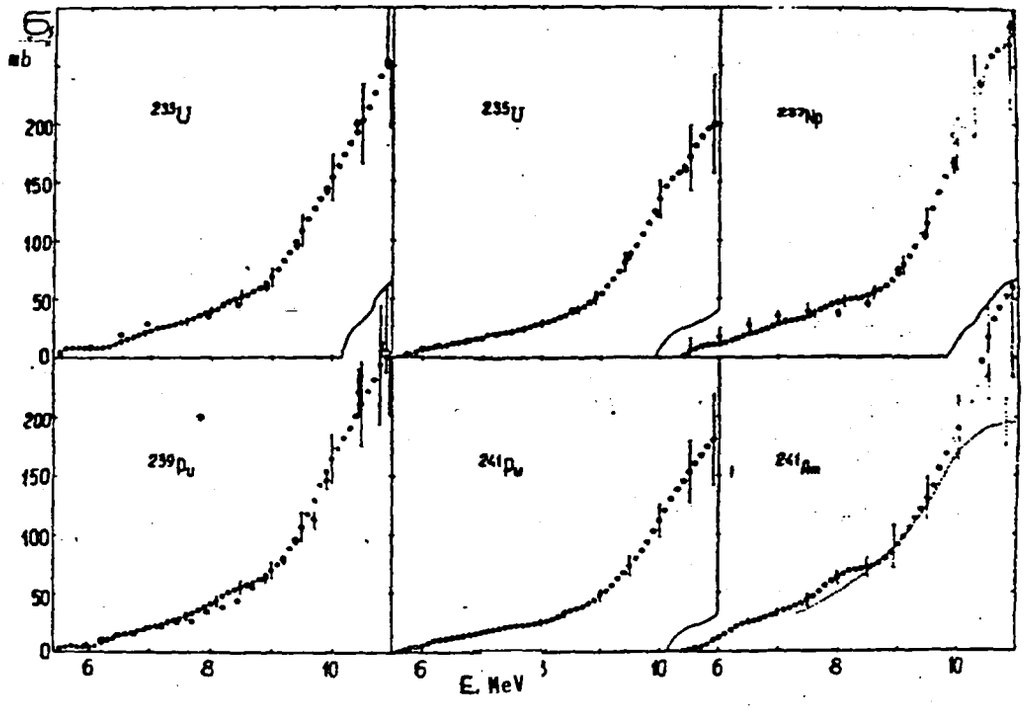

Fig. 4. Photofission cross-sections σ_f as a function of photon energy E. Experimental data: o - present study, ⊗ - Refs [8, 18]. ..... - Ref. [19].